

Ab-initio study of $\text{Ti}_3\text{Si}_{0.5}\text{Ge}_{0.5}\text{C}_2$ under pressure

W. Orellana^a, G. Gutiérrez^a, E. Menéndez-Proupin^a,
J. Rogan^a, G. García^b, B. Manoun^c, S. Saxena^c

^a*Departamento de Física, Facultad de Ciencias, Universidad de Chile, Casilla 653, Santiago, Chile.*

^b*Facultad de Física, P. Universidad Católica de Chile, Casilla 307, Santiago 2, Chile.*

^c*Center for Study of Matter at Extreme Conditions (CeSMEC), Florida International University, VH-140, University Park, Miami, Florida 33199*

Abstract

Structural and electronic properties of $\text{Ti}_3\text{Si}_{0.5}\text{Ge}_{0.5}\text{C}_2$ under pressure up to 80 GPa are studied by means of first principles calculation based on density functional theory (DFT). The total energy, lattice parameters and atomic positions are employed to investigate the structural changes under pressure. Within the local density approximation (LDA) used in the calculation, the obtained equilibrium volume and the bulk modulus are in good agreement with the experimental values. The compression is almost isotropic up to 15 GPa, but above this pressure a certain degree of anisotropy appears. The calculated electronic properties reveals that the band structure and the density of states (DOS) do not present big changes under pressure. However, it is noticeable a decrease of the DOS at the Fermi level under pressure, which could result in a reduction of the electrical conductivity at high pressure.

Key words: MAX Phases, high pressure, structural properties, electronic properties, first principles calculation

PACS: 62.50.+p, 1.20.Be, 71.20.Be, 64.30.+t, 71.15.Mb

Email address: gutierr@fisica.ciencias.uchile.cl (G. Gutiérrez).

URL: <http://fisica.ciencias.uchile.cl/~gutierr> (G. Gutiérrez).

1 Introduction

The quaternary $\text{Ti}_3\text{Si}_{0.5}\text{Ge}_{0.5}\text{C}_2$ compound belongs to the thermodynamically stable nanolaminates, so called MAX phases. These materials are made up of an early transition metal M, an element (or a mixture of them) from the A groups, usually IIIA and IVA, and a third element, X, which is either nitrogen or carbon, in the composition $\text{M}_{n+1}\text{AX}_n$, where n is 1, 2 or 3. These ternary carbides and nitrides combine unusual properties of both metals and ceramics. Like metals, they are good thermal and electrical conductors as well as relatively soft. Like ceramics, they are elastically stiff and some of them, such as Ti_3SiC_2 , Ti_3AlC_2 and Ti_4AlN_3 , also exhibit excellent high temperature mechanical properties. They are resistant to thermal shock and unusually damage tolerant, exhibiting excellent corrosion resistance. Above all, unlike conventional carbides or nitrides, they can be machined by conventional tools without lubricant, which is of great technological importance for the application of the MAX phases. Up to now there are roughly fifty M_2AX phases, four M_3AX_2 and only one M_4AX_3 phases known [1]. $\text{Ti}_3\text{Si}_{1-x}\text{Ge}_x\text{C}_2$, being an isoelectronic alloy, offers the possibility to probe the influence of the metallic character of the A element on the physical properties. This has recently been shown for the magnetoelectric, thermal and elastic properties at low temperature [2].

For the application of MAX phases as structural materials it is essential to deeply understand its properties and how they are related to the atomic scale and the electronic structure. Several *ab-initio* calculations of the electronic structure of the representative material Ti_3SiC_2 have been reported in the last five years [3–8] with applications to mechanical properties, structural stability, lattice dynamics, and polymorphism. The electronic structure has been reported for other M_3AX_2 compounds, such as Ti_3GeC_2 [6,9,10], Ti_3AlC_2 [6,11], and the solid solution $\text{Ti}_3\text{Si}_{0.75}\text{Al}_{0.25}\text{C}_2$ [12]. Elastic properties of $\text{Ti}_3\text{Si}_{1-x}\text{Ge}_x\text{C}_2$ solid solutions are reported in Ref. [2]. It is also essential to describe how these properties may change under pressure. In spite of its importance, only a few studies about M_3AX_2 phases under pressure exist. In particular, to the best of our knowledge, the only work on $\text{Ti}_3\text{Si}_{0.5}\text{Ge}_{0.5}\text{C}_2$ under pressure is the experiment performed by Manoun *et al.* [13]. For the end members of this compound there are some experimental [14–16] and theoretical works [17,3].

Using synchrotron x-ray diffraction measurements, Onodera *et al.* [14] showed that Ti_3SiC_2 is structurally stable up to 61 GPa. They found a bulk modulus of 206 ± 6 GPa and that the decrease of the c -axis length is faster than that of the a -axis length. A recent theoretical *ab-initio* calculation by Wang *et al.* [3], in the framework of density functional theory (DFT) within the local density approximation (LDA) complement this information. These authors

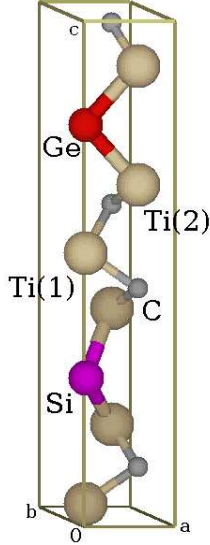


Fig. 1. (Color online) $\text{Ti}_3\text{Si}_{0.5}\text{Ge}_{0.5}\text{C}_2$ unit cell used in this work.

found that Ti_3SiC_2 exhibits elastic anisotropy up to 110 GPa. Examining the bond lengths contraction at different pressures and relating it with a Mulliken population analysis, they concluded that the Ti–Si bond possesses the weakest covalent bonding strength. The Ti–C bond is less weak, and finally the Ti–Ti ionic bonding is the stiffest one. In addition, although the electronic structure does not suffer a big change, it is clearly observable a decrease of the density of states (DOS) at the Fermi level according the pressure increases. This fact implies a decrease of the electrical conductivity in Ti_3SiC_2 under pressure. For Ti_3GeC_2 , the structural and chemical analog Ti_3SiC_2 , a recent experimental work report that this compound present a pressure–induced phase transformation at 26.6 GPa. However, in contrast to these results, new measurements has not found evidence of phase transformation up to 51 GPa [16]. The discrepancy may be due to a different stress state in the experiment.

In this paper we present a first principles study on the structural and electronic properties of $\text{Ti}_3\text{Si}_{0.5}\text{Ge}_{0.5}\text{C}_2$ under pressure up to 80 GPa. The energy–volume and pressure–volume as well as the cell parameters relation respect to pressure are employed to study the changes of the structural properties under pressure. Regarding the electronic properties, we analyze the band structure and the changes in the electronic density of states induced by pressure. Bonding properties are analyzed by means of the charge density contour plots.

2 Calculation method

$\text{Ti}_3\text{Si}_{0.5}\text{Ge}_{0.5}\text{C}_2$, like Ti_3SiC_2 and Ti_3GeC_2 , has an hexagonal structure with space group $P6_3/mmc$. The experimental lattice constants[13] are $a = 3.079 \text{ \AA}$ and

Table 1

Experimental and calculated volume V_0 , bulk modulus B and B'_0 for $\text{Ti}_3\text{Si}_{0.5}\text{Ge}_{0.5}\text{C}_2$. The letters in parenthesis, M and B-M, stands for Murnaghan and Birch-Murnaghan fit, respectively.

	V_0 (\AA^3)	B_0 (GPa)	B'_0
Experiment (M)	145.9	185 ± 5	3.0 ± 0.3
Experiment (B-M)	145.9 ± 0.1	183 ± 4	3.4 ± 0.2
DFT-LDA (M)	133.78 ± 0.06	208 ± 2	3.65 ± 0.05
DFT-LDA (B-M)	133.84 ± 0.05	204 ± 2	4.05 ± 0.05

$c = 17.77$ \AA . Figure 1 shows a $\text{Ti}_3\text{Si}_{0.5}\text{Ge}_{0.5}\text{C}_2$ structure which contains 12 atoms per unit cell, that is, two formula units per unit cell. This arrangements of atoms can be described as two layers of edge-sharing Ti_6C octahedron interleaved by a two dimensional close packed Si or Ge layer. Notice that this is one out of several possible realizations of this compound. For example, it is possible to enlarge the unit cell in order to distribute the Si and Ge in different ways, but keeping the correct stoichiometry. In this work we calculate the structural and electronic properties of $\text{Ti}_3\text{Si}_{0.5}\text{Ge}_{0.5}\text{C}_2$ under pressure using two different supercells: a 12 atoms supercell, corresponding to Figure 1, and a supercell of 24 atoms, where the Si and Ge atoms are mixed in the same layer. Interestingly, the results of the calculation using these two models show no significant differences. Therefore, here we report in detail only the results corresponding to the supercell of 12 atoms.

The calculations were performed in the framework of the density functional theory (DFT) [18], using a basis set of strictly-localized numerical pseudoatomic orbitals as implemented in the SIESTA code [19], The exchange-correlation energy is calculated within the local density approximation (LDA) [20]. Standard norm-conserving pseudopotentials [21] in their fully separable form [22] are used to describe the electron-ion interaction. We consider a double- ζ singly-polarized (DZP) basis set. For the Brillouin zone sampling we use a Monkhorst-Pack mesh of $7 \times 7 \times 2$ special k points [23]. Hydrostatic pressure coupled with the variable cell approach were applied within the Parrinello-Rahman method [24]. In this way, for each target pressure a full optimization of the cell shape and atom positions is performed.

3 Results

Figure 2a) shows the energy as a function of the volume, together with the corresponding fit to the Murnaghan equation [25]. In Figure 2b) pressure-volume relation are displayed, both the theoretical calculations (Murnaghan

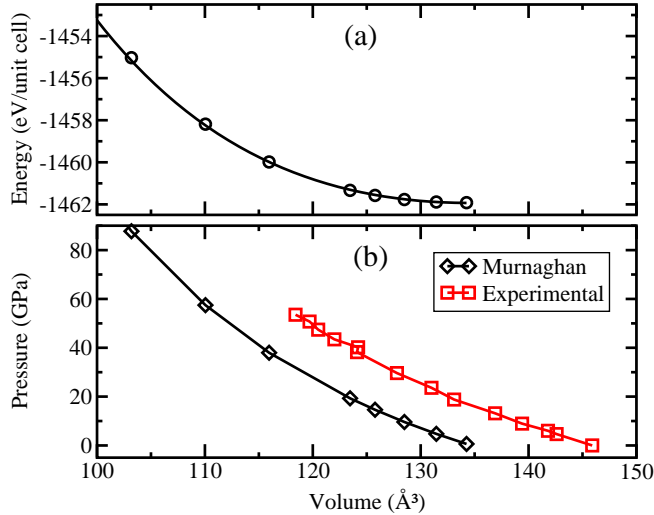


Fig. 2. (Color online) Equation of state of $\text{Ti}_3\text{Si}_{0.5}\text{Ge}_{0.5}\text{C}_2$ under pressure. (a) Energy versus volume. The solid line correspond to the fit of *ab-initio* results to the Murnaghan equation. (b) Pressure versus volume.

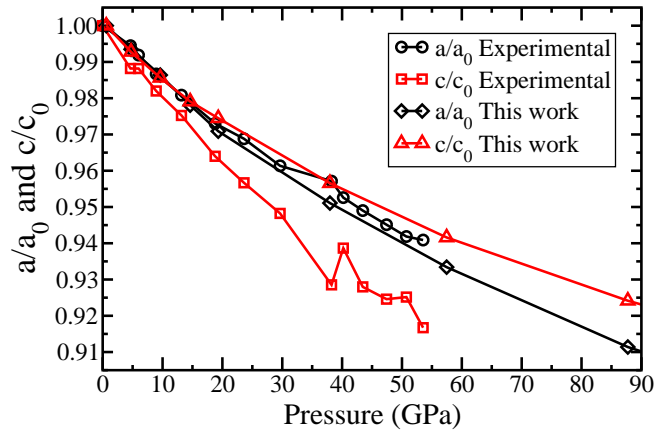


Fig. 3. (Color online) Cell parameters according pressure. a_0 and c_0 indicate the equilibrium value at zero pressure.

fit) as well as the experimental results [13]. It can be seen that the calculated equilibrium volume at ambient pressure is 8% smaller than the experimental one, which is a well known trend of DFT–LDA calculation. From these curves we determined the bulk modulus. By using the Murnaghan equation we obtain a value of 208 ± 2 GPa for the bulk modulus with $B'_0 = 3.65 \pm 0.05$ and an equilibrium volume of $133.78 \pm 0.06 \text{ \AA}^3$. Fitting the same data to the Birch–Murnaghan equation [26], the resulting bulk modulus is 204 ± 2 GPa. These values are slightly greater than the experimental bulk modulus, 183 ± 4 GPa, obtained by fitting the Birch–Murnaghan equation. Performing a Murnaghan fit on the experimental data we obtained a value of 185 ± 5 GPa. Table 1 presents a summary with these results.

The variation of the normalized lattice constant a/a_0 and c/c_0 with pressure is

Table 2

Interatomic distances and angles of $\text{Ti}_3\text{Si}_{0.5}\text{Ge}_{0.5}\text{C}_2$ at two different pressures.

	0 GPa	80 GPa
Distances (Å)		
Ti–Ge	2.68	2.42
Ti–Si	2.63	2.38
Ti–C	2.11	1.93
Ti–Ti	2.88	2.72
Angles (°)		
Ti–Ge–Ti	99.4	98.8
Ti–Si–Ti	97.9	96.4
Ti–C–Ti	87.9	89.4

shown in Figure 3. Also, the values of the experimental lattice constant under pressure are displayed. The calculated lattice constants at zero pressure are $a = 2.991 \text{ \AA}$ and $c = 17.318 \text{ \AA}$, slightly smaller than the experimental ones. The relative ratio $(c/a)/(c_0/a_0)$ of the calculated lattice constants is approximately one for pressures below 15 GPa, but above this pressure that ratio is greater than one. Thus, according to our findings, the compound compress in an isotropic way when the external pressure is less than 15 GPa. However, over this pressure, the compound is slightly stiffer in the perpendicular direction to the basal plane than that of the parallel direction to the basal plane. This behavior contrast to the experiment, where $(c/a)/(c_0/a_0) \leq 1$ up to 61 GPa. The observed difference between the theoretical and the experimental results could be attributed to the fact that in the experiment the application of pressure is not done in a fully hydrostatic way, as it is performed in the calculation. Notice that for Ti_3SiC_2 there is also a discrepancy between the ab-initio and the experimental results in this respect. Whereas in the experiment [14] $(c/a)/(c_0/a_0) \leq 1$ from 0 to 61 GPa, the calculated $(c/a)/(c_0/a_0)$ ratio is less than one only for pressures between 0–30 GPa, but is greater than one for pressure above 40 GPa [3].

Further insight about the change of the structural properties under pressure can be obtained by analyzing the bond lengths and bond angles, which are shown in Table 2. It is known that in Ti_3SiC_2 and Ti_3GeC_2 the Ti atoms are located in two non-equivalent position corresponding to Wyckoff positions 2a and 4f, called Ti(1) and T(2) respectively. In Ti_3SiC_2 at zero pressure the Ti(1)–C bond length is 2.181 \AA and Ti(2)–C= 2.085 \AA . These values are similar to the average value that we obtained for $\text{Ti}_3\text{Si}_{0.5}\text{Ge}_{0.5}\text{C}_2$, of 2.11 \AA . In the same way, the calculated Ti–Ge and Ti–Si bond lengths are also similar to the Ti–Si value in Ti_3SiC_2 , 2.693 \AA [1].

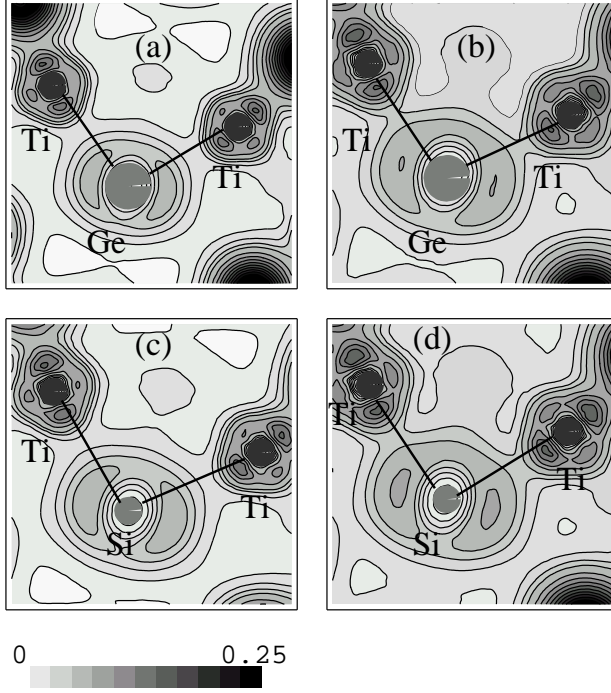


Fig. 4. Charge density contour plots for $\text{Ti}_3\text{Si}_{0.5}\text{Ge}_{0.5}\text{C}_2$ through planes passing by the Ti-Ge-Ti and Ti-Si-Ti bonds. (a) and (c) are plots at zero pressure and (b) and (d) are the corresponding plots at 80 GPa.

We can evaluate the relative bonding strength of $\text{Ti}_3\text{Si}_{0.5}\text{Ge}_{0.5}\text{C}_2$ by comparing the contraction of the bond lengths according to pressure. The most compressible bonds are the Ti-Ge and the Ti-Si, which decrease by 10% and 9.6%, respectively, when the pressure reach 80 GPa. These bonds have a covalent character. The Ti-C bond length decrease by 8% at 80 GPa with respect to its length at zero pressure, whereas the Ti-Ti bond length, which has an ionic character, is the stiffest one, shrinking only by 5% when the pressure changes from 0 to 80 GPa.

The above description is consistent with an electronic level analysis. Figure 4 shows the charge density along the Ti-Ge and Ti-Si bond direction at pressures of 0 and 80 GPa. It can be seen that the effect of pressure is to increase the charge overlap between atoms, which tends to spread out through the cell. This observation is in agreement with the results for Ti_3SiC_2 under pressure [3].

Finally, we investigate the electronic properties of $\text{Ti}_3\text{Si}_{0.5}\text{Ge}_{0.5}\text{C}_2$ by means of the band structure and the density of states (DOS). Figure 5 displays the band structure and the DOS at the pressures of 0 GPa and 80 GPa. It can be observed that there are not major changes either in the bands structure or in the DOS at pressures up to 80 GPa. The conduction band and the valence band are still overlapping, thus the metallic character remains in this

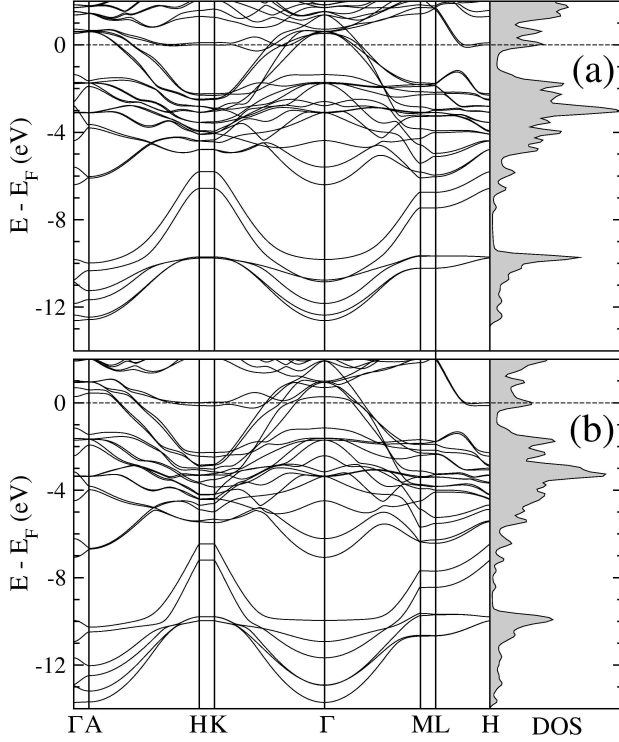


Fig. 5. Electronic band structure along the high symmetry direction of the BZ and total density of states (DOS) for $\text{Ti}_3\text{Si}_{0.5}\text{Ge}_{0.5}\text{C}_2$ at zero pressure (a), and at 80 GPa (b).

compounds. But in the DOS it should be noted that at 80 GPa there is a decrease of the density of states at the Fermi level with respect to 0 GPa. This trend, similar as the case of Ti_3SiC_2 under pressure, could result in a reduction of the electrical conductivity of $\text{Ti}_3\text{Si}_{0.5}\text{Ge}_{0.5}\text{C}_2$ under pressure.

4 Concluding remarks

In summary, we have investigated the structural changes and the electronic properties of the nanolaminate compound $\text{Ti}_3\text{Si}_{0.5}\text{Ge}_{0.5}\text{C}_2$ at eight different pressures, from 0 to 80 GPa in a fully hydrostatic way. The calculated equilibrium volume is 8% smaller than its experimental value, whereas the bulk modulus is almost 10% greater than its experimental counterpart. Both facts are a well-known trend of DFT-LDA calculation. By analyzing the effects of compression on the interatomic distances, we were able to classify the different bond strengths from the weakest to the stiffest ones, in the order Ti–Ge, Ti–Si, Ti–C and Ti–Ti, respectively. This is analog to the case of Ti_3SiC_2 . Interestingly, according our findings, there is almost no anisotropy under compression up to 15 GPa, but above this pressure the relative decrease of the c-axis is less than the relative decrease of the basal axis, in contrast to the experimental

results. Regarding to the electronic properties, the band structure and the density of states (DOS) do not present big changes under pressure. Nevertheless, the physical properties which depend on the DOS at the Fermi level change under pressure, because at 80 GPa the DOS at the Fermi level is smaller than the DOS at the Fermi level at ambient pressure. In particular the electrical conductivity could decrease.

Acknowledgments

W. O. and G. G. thank to Millennium Nucleus (MIDEPLAN and CONICYT), Applied Quantum Mechanics and Computational Chemistry project No. P02-004-F (W. O.), and Condensed Matter project P02-054-F (G. G.), for financial support. G. G., E. M-P., and J. R. are supported by FONDECYT (Chile), grants 1030063, 1050293, 1030957, respectively. This work was also financially supported by a grant from the National Science Foundation (DMR 0231291). Computer time of MAIDROC at FIU is gratefully acknowledged.

References

- [1] M. W. Barsoum, *Prog. Solid. St. Chem.* **28**, 201 (2000).
- [2] P. Finkel, B. Seaman, K. Harrell, J. Palma, J. D. Hettinger, S. E. Lofland, A. Ganguly, M. W. Barsoum, Z. Sun, Sa Li, and R. Ahuja, *Phys. Rev. B* **70**, 085104 (2004).
- [3] J. Y. Wang, and Y. C. Zhou, *J. Phys.: Condens. Matter* **15**, 1983 (2003).
- [4] Y. C. Zhou, Z. M. Sun, *J. Phys.: Condens. Matter* **12**, L457 (2000).
- [5] B. Holm, R. Ahuja, and B. Johansson, *Appl. Phys. Lett.* **79**, 1450 (2001).
- [6] Y. C. Zhou, Z. M. Sun, X. H. Wang, *et al.*, *J. Phys.: Condens. Matter* **13**, 10001 (2001).
- [7] J. Y. Wang, and Y. C. Zhou, *Phys. Rev. B* **69**, 144108 (2004).
- [8] J.-P. Palmquist, S. Li, P.-O.-Å Persson, J. Emmerlich, O. Wilhelmsson, H. Högberg, M. I. Katsnelson, B. Johansson, R. Ahuja, O. Eriksson, L. Hultman, and U. Jansson, *Phys. Rev. B* **70**, 165401 (2004).
- [9] Z. M. Sun, and Y. C. Zhou, *J. Mater. Chem.* **10**, 343 (2000).
- [10] Y. C. Zhou, and Z. M. Sun, *J. Appl. Phys.* **86**, 1430 (1999).
- [11] Y. C. Zhou, X. H. Wang, Z. M. Sun, S.Q. Chen, *J. Mater. Chem.* **11**, 2339 (2001).

- [12] J. Y. Wang, and Y.C. Zhou J. Phys.: Condens. Matter. **15** 5968 (2003).
- [13] B. Manoun, H. P. Liermann, R. Gulve, S. K. Saxena, A. Ganguly, M. W. Barsoum, and C. S. Zha, Appl. Phys. Lett. **84**, 2799 (2004).
- [14] A. Onodera, H. Hirano, T. Yuasa, N. F. Gao and Y. Miyamoto, Appl. Phys. Lett. **74**, 3782 (1999).
- [15] Z. Wang, C. S. Zha, and M. W. Barsoum, Appl. Phys. Lett. **85**, 33453 (2004).
- [16] B. Manoun, H. Yang, R. P. Gulve, S. K. Saxena A. Ganguly, M. W. Barsoum, and C. S. Zha, *unpublished*.
- [17] Z. Sun, and Y. C. Zhou, J. Mater. Chem. **10**, 342 (2000).
- [18] W. Kohn, Rev. Mod. Phys. **71**, 1253 (1999).
- [19] P. Ordejón, E. Artacho, and J. M. Soler, Phys. Rev. B **53**, R10441 (1996); J.M. Soler, E. Artacho, J. D. Gale, A. García, J. Junquera, P. Ordejón, D. Sánchez-Portal, J. Phys.: Condens. Matter **14**, 2745 (2002).
- [20] J. P. Perdew and A. Zunger, Phys. Rev. B **23**, 5048 (1981).
- [21] N. Troullier and J. L. Martins, Phys. Rev. B **43**, 1993 (1991).
- [22] L. Kleinman and D. M. Bylander, Phys. Rev. Lett. **48**, 1425 (1982).
- [23] H. J. Monkhorst and J. D. Pack, Phys. Rev. B **13**, 5188 (1976).
- [24] M. Parrinello and A. Rahman, Phys. Rev. Lett. **45**, 1196 (1980); J. Appl. Phys. **52**, 7182 (1981).
- [25] F. D. Murnaghan, Proceedings of the National Academy of Sciences, **30**, 244 (1944).
- [26] F. Birch, Phys. Rev. **71**, 809 (1947).